3rd Specialty Conference on Material Engineering & Applied Mechanics
3e Conférence spécialisée sur le génie des matériaux et mécanique appliquée

Montréal, Québec
May 29 to June 1, 2013 / *29 mai au 1 juin 2013*

MEC-4

Vibration Suppression and Buckling Control of a Smart Piezoelectric Composite Plate

Q.S. Wang
Department of Civil Engineering and Applied Mechanics, McGill University

Abstract: Both vibration suppression and buckling control of a fibre-reinforced composite plate using a distributed surface bonded PZT piezo-ceramic sensor and actuator are studied in this paper. A C0 continuous, shear flexible, eight-node serendipity doubly curved plate/shell element is first developed based on the layer-wise shear deformation theory, linear piezoelectric mechanical coupled constitutive relations, and Hamilton variation principle. This element has considered the stiffness, mass, and electromechanical coupling effects of the piezoelectric sensor and actuator layers. Then, approximate reduced modal models are derived by using the finite element vibration and buckling analyses results of the piezo-laminated plate and the approximate linear quadratic Gaussian (LQG) compensator singular values. Next, state space modal models which integrated the host composite plate with bonded piezoelectric sensor and actuator layers are implemented and used to design a linear quadratic regulator (LQR) controller, a dynamic state observer, and an LQG compensator to achieve the controls. The designed LQR/LQG controls are shown to be successful in suppressing the vibrations for an impulse/a random excitation and stabilizing the first buckling mode of the smart composite plate.

Keywords: Piezoelectric; Vibration suppression; Buckling control; Distributed sensor and actuator; Smart composite plate;

1 Introduction

Smart structures have been developed to achieve active vibration suppression and have seen many applications in aerospace, automotive, and civil engineering, see Chopra (2002). Law et al. (2003) presented an adaptive vibration control of piezoelectric laminated structures. Kusculuoglu and Royston (2005) developed a four-node Lagrange and an eight-node Serendipity quadratic element for the vibration control of piezo-laminated plates. Polit and Bruant (2006) presented an eight-node plate element and the electric potential was approximated using the layer-wise approach. Balamurugan and Narayanan (2001) and Narayanan and Balamurugan (2003) developed a shear flexible, nine-node quadrilateral shell element based on field consistency principle and applied for the vibration control of piezo-laminated smart structures. Compare to the much work done on the vibration control, the buckling control of smart structures due to an axial load has lacked attention. A finite-element model was developed for the active buckling control of piezo-laminated composite plates with integrated sensors and actuators by Chandrashekhara and Bhatia (1992). Meressi and Paden (1993) analytically showed that the buckling of a flexible beam can be postponed beyond the critical load by means of feedback control using piezoelectric actuators and strain gauge sensors. Further research completed by Varelis and Saravanos (2004) incorporated nonlinear effects due to large rotations to predict the buckling and post-buckling response of adaptive composite beams and plates.

While many finite element models have been developed for the vibration and buckling analyses of piezoelectric smart structures, the active buckling control design of piezo-laminated plates and shells, as well as the integration of both dynamic modal analysis and feedback control design for the vibration suppression and buckling control have been absent. In this paper, approximate reduced modal models are derived by using the finite element vibration and buckling analysis results and the approximate linear quadratic Gaussian (LQG) compensator singular values. Then linear quadratic regulator (LQR) controllers, dynamic state observers, and LQG compensators are designed to achieve both the vibration and buckling controls of a smart composite plate.

2 Formulation

A C0 continuous, shear flexible, eight-node serendipity doubly curved shell element is developed based on the layer-wise shear deformation theory, linear piezoelectric mechanical coupled constitutive relations, and Hamilton variation principle for the piezo-laminated smart composite plate/shell. The displacement field in kth layer is

[1] $u_1^k(x,y,z) = \left(1+\frac{z}{R_x}\right)u^k(x,y) + z\emptyset_x^k(x,y)$
$u_2^k(x,y,z) = \left(1+\frac{z}{R_x}\right)v^k(x,y) + z\emptyset_y^k(x,y)$
$u_3^k(x,y,z) = w(x,y)$

where (u^k, v^k, w) are the mid-plane displacement; (u_1, u_2, u_3) are the displacement components in the x, y, z directions; $\emptyset_x^k, \emptyset_y^k$are the rotations in kth layer; $R_x, R_y$are constant principal radii of curvature with $R_x = R_y = \infty$ for the plate.

Using the eight-node Serendipity iso-parametric quadrilateral shell element to discrete the displacement field and applying the linear piezoelectric constitutive equations, the element dynamic governing equations can be derived by using Hamilton's principle. (See Wang, Qishan 2012)

After assembly of element matrices and vectors and adding of the damping term, the global governing equation can be written as:

[2] $[M]\{\ddot{U}\} + [C_d]\{\dot{U}\} + [K_{UU}]\{U\} + \left[K_{UQ}^a\right]\{Q^a\} + \left[K_{UQ}^s\right]\{Q^s\} = \{F_M\}$

where$[M], [C_d], [K_{UU}], K_{UQ}^a, K_{UQ}^s$, and $F_M$are the mass, damping, mechanical stiffness, coupling stiffness of actuator, coupling stiffness of sensor and mechanical force vector, respectively; $\{Q^a\}$ and $\{Q^s\}$ are the actuator charge and sensor charge.

After substituting the actuator charge and sensor charge, the global governing equation can be written as:

[3] $[M]\{\ddot{U}\} + [C_d]\{\dot{U}\} + [K^*]\{U\} = \{F_M\} - [K^a]\{\Phi_a\}$

where $\{\Phi_a\}$ is the actuator applied voltage; details of the $[K^*]$ and $[K^a]$ are given in Wang, Qishan (2012).

For the buckling analysis of the piezoelectric laminated plate and shell, the global buckling equation is:

[4] $[M]\{\ddot{U}\} + [C_d]\{\dot{U}\} + [K^*]\{U\} - P[K_G]\{U\} = \{F_M\} - \{K^a\}\{\Phi_a\}$

where $[K_G]$ is the geometric stiffness and P is the in-plane buckling load.

3 Results and Discussion

Active controls of both vibration and buckling of the same cantilevered laminated composite plate are studied. As shown in Figure 1, a graphite/epoxy composite cantilever plate ($Rx = Ry = \infty$) with PZT piezoceramic senor and actuator bonded to both the upper and lower surfaces is considered. The plate consists of four composite layers $(-45°/45°/-45°/45°)$ of $2.5mm$ thickness each. The two outer piezoelectric layers are of $h_a = h_s = 0.1mm$ thickness each. The material properties are as in Table 1.

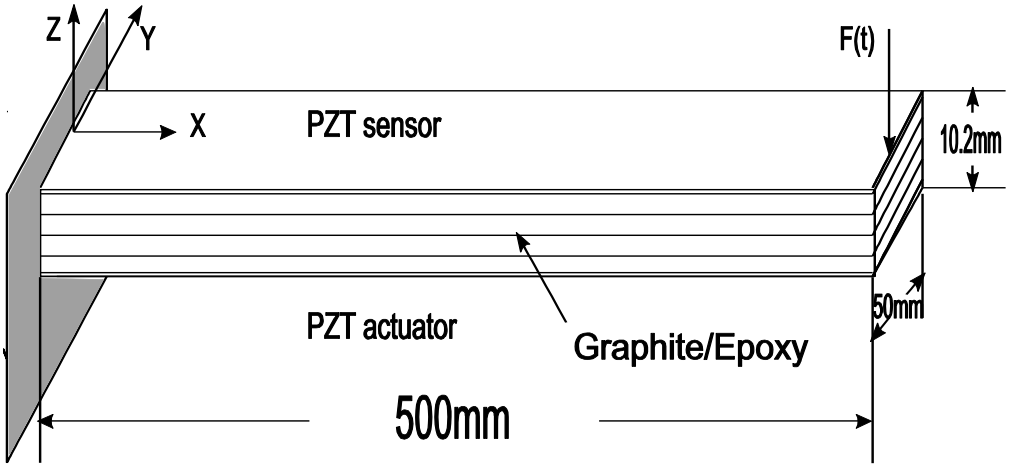

Figure 1: A composite cantilever plate with distributed PZT sensor and actuator

Table 1: Graphite/epoxy, PZT piezo-ceramic and Steel material properties (See Wang, Qishan 2012)

Properties	Piezo-ceramic PZT-G1195N	Graphite/epoxy T300/976	Steel
Elastic modulus $E_{11}(Pa)$	63.0×10^9	150.0×10^9	2.1×10^{11}
Elastic modulus $E_{22} = E_{33}(Pa)$	63.0×10^9	9.0×10^9	2.1×10^{11}
Shear modulus $G_{12}(Pa)$	24.2×10^9	7.1×10^9	--
Shear modulus $G_{13} = G_{23}(Pa)$	24.2×10^9	2.5×10^9	--
Poisson's ratio $\nu_{12} = \nu_{13} = \nu_{23}$	0.3	0.3	0.3
Density $\rho(Kg/m^3)$	7600.0	1600.0	7800.0
Electric permittivity $\epsilon_{11} = \epsilon_{22}(F/m)$	1.53×10^{-8}	--	--
Electric permittivity $\epsilon_{33}(F/m)$	1.50×10^{-8}	--	--
Piezoelectric strain constant $d_{31} = d_{32}(m/V)$	$\mathbf{2.54 \times 10^{-10}}$	--	--
Maximum electric field (V/μm)	$\mathbf{1.0}$	--	--

3.1 Active Vibration Suppression

This case was also studied by Balamurugan and Narayanan (2001). In their paper, a nine-node quadrilateral shell element was derived and different classical control laws, including constant gain negative velocity feedback, direct proportional feedback and Lyapunov feedback are applied to compare the vibration control performance. As shown here, consistent results are obtained.

Table 2 shows the first six natural frequencies comparison. The first four modes are well matched, only the two higher modes shift away as the different element discretion. Also the first four mode shapes are showed in Figure 2.

Table 2: The first six natural frequencies (Hz) for a cantilever composite plate

Mode	Q9 plate/shell element (Balamurugan and Narayanan 2001)	Q8 plate/shell element (40×4)
1	27.05	26.3616
2	127.11	123.8683
3	169.17	164.1050
4	475.86	455.8193
5	780.64	640.6344
6	797.76	761.5805

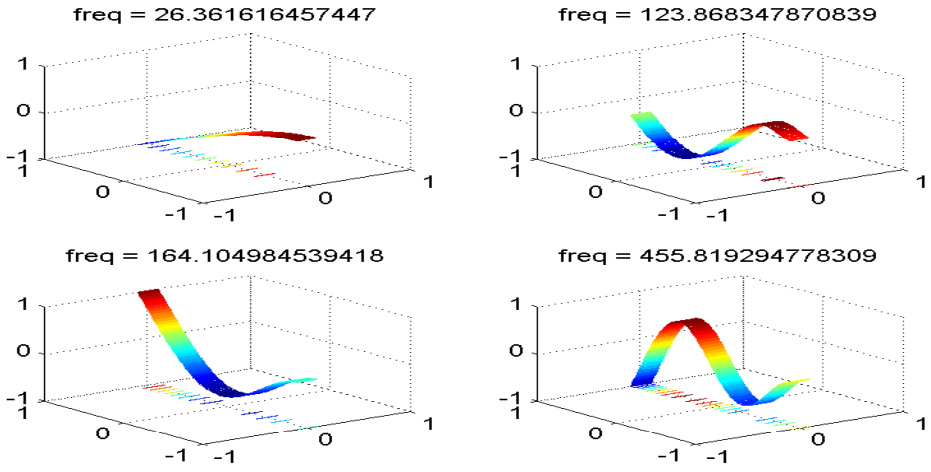

Figure 2: First four vibration modes of a composite cantilever plate (HZ)

To design the LQR/LQG controllers and compensators for this more complex composite laminated plate case, first we have to determine the smallest states model which can keep an accurate representation of the frequency response characteristics.

Suppose the first six modes are chosen to build an approximate reduced model. Then a balanced LQG state space representation can be given. By the definition of the ``LQG-balanced representation'', (see Gawronski 1994) $\lambda_i, i = 1, \ldots 6$ are LQG singular values of the structure system and its approximate LQG singular values$\lambda_{approx} = \sqrt{P_c{}^T P_c * P_e P_e{}^T}$, P_c is the solution of the Controller Algebraic Riccati Equation

(CARE) and P_e is the solution of the Filter Algebraic Riccati Equation (FARE). Also Hankel singular values can be obtained as $\gamma = G_c G_o$, G_c is the control Grammian and $G_o$is observer Grammian. (See Lewis and Syrmos 1995).Then the approximate reduced LQG compensator singular values $\sigma_{approx} = \gamma \times \lambda_{approx}$ can be obtained.

Figure 3 shows the three singular values sorted in increasing or decreasing order. It can be seen that the approximate LQG singular values of the reduced model are the same as the LQG singular values of the structure system and this means that the six modes reduced model can accurately represent the full states finite element model. Furthermore, the sorted approximate LQG compensator singular values show that only the first mode has a large contribution to the impulse response of the tip displacement, the other modes can be reduced.

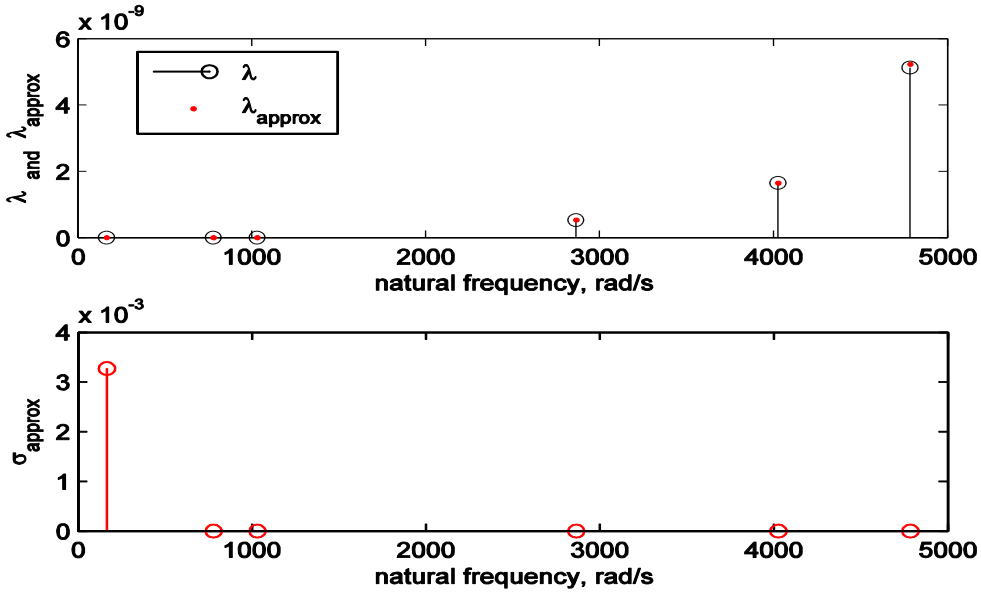

Figure 3: LQG/approximate LQG singular values and approximate LQG compensator singular values

Next, only the first mode is used to design an LQR/LQG compensator to control the vibration of the cantilever composite plate. An impulse load of 0.1N is applied at the free end of the plate. The dynamic response is calculated by using only the first mode. As in the study by Balamurugan and Narayanan (2001), the damping is ignored. In a real case situation, the damping will also contribute its part of vibration stabilization. Here only the active control effect is expected and shown.

To design an LQR/LQG compensator, we have one mode (or two states) least reduced model to control. As the derivative of the sensor output is assumed to be able to be computed, with one surface bonded sensor and one surfaced bonded actuator, a full state feedback LQR controller can be designed. While the tip vertical displacement is set as performance output, the state weight matrix Q can be computed from output matrix C with $Q = C^T C$ and control parameters are taken as $\alpha = 10^4$ and $\beta = 1$.

Figure 4 shows the impulse response of the plate's tip displacement, for which the control is started after a lapse of 0.5s in order to compare both the controlled and uncontrolled responses. It shows good agreements with the study by Balamurugan and Narayanan (2001). The corresponding frequency response of the uncontrolled and controlled tip displacement is shown in Figure 5.

The sensor output voltage and the actuator control voltage are shown in Figures 6 and 7. It is seen that the actuator control voltage has an absolute value less than the breakdown voltage ($V_{max} = h_a \times 1.0v/\mu m = 100v$) of the piezoelectric PZT-actuator. The designed LQR/LQG controller has suppressed the vibration of the plate under the tip impulse load.

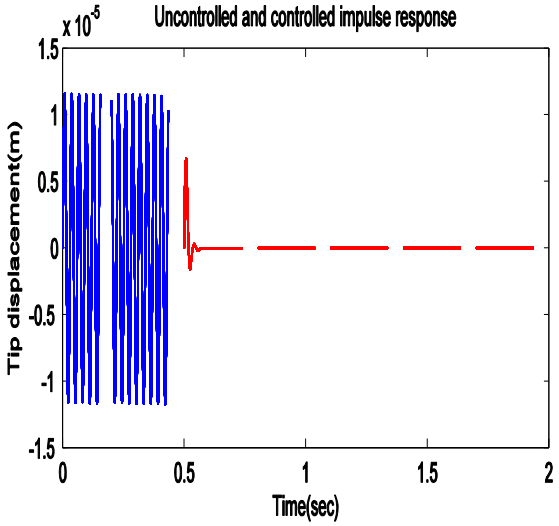

Figure 4: Tip displacement of the plate

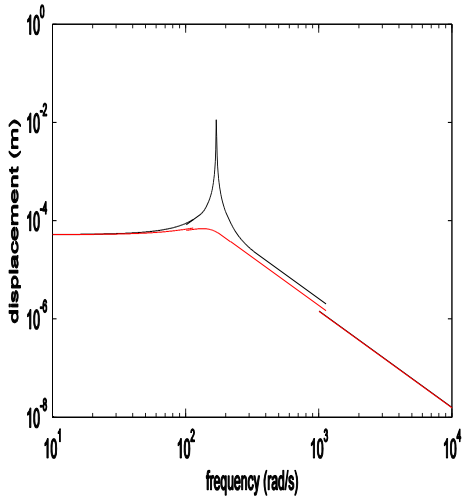

Figure 5: Frequency responses of the plate

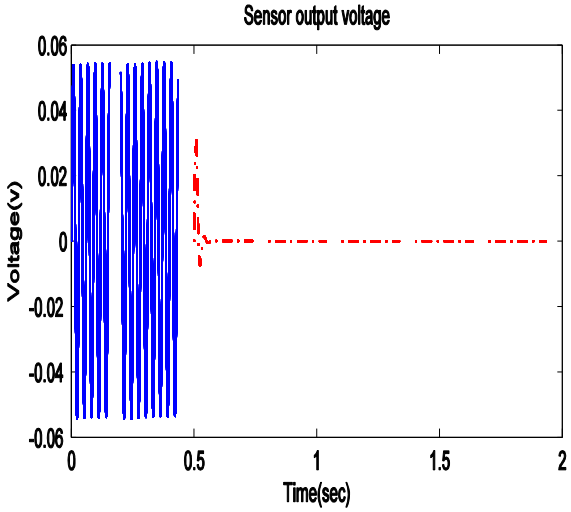

Figure 6: Sensor output of plate}

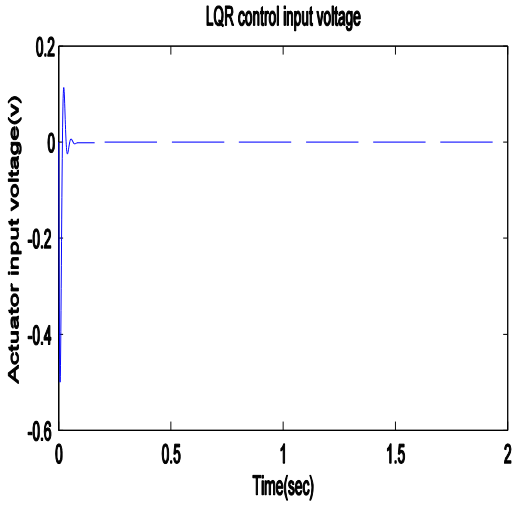

Figure 7: Actuator control input voltage

Next the active vibration control of the plate subjected to random loading is studied. The random load as in Figure 8, which is a band limited white noise of Power Spectral Density PSD=1.1722×$10^{-6}N^2/(rad/s)$ in the frequency range of 0-1000Hz, is applied on the tip of the cantilever plate. The uncontrolled and controlled responses at the free end of the plate are shown in figures 9 and 10. The Mean Square Response (MSR) for the both uncontrolled and controlled cases are 7.4421×10^{-8} and 2.0486×10^{-10} respectively. The MSR reduction factor is about 363, which indicates that the distributed sensors and actuators are effective in controlling the random vibration also.

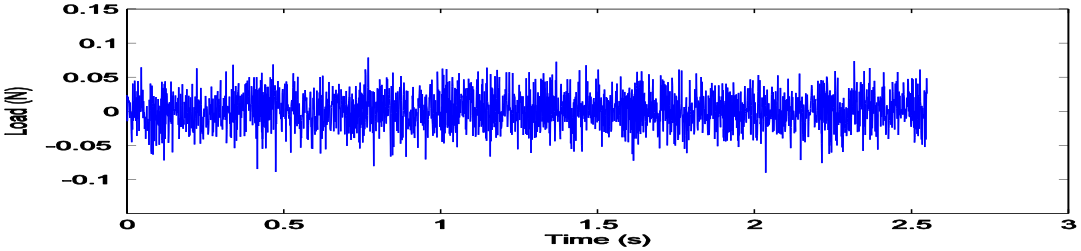

Figure 8: Random load history in the frequency range of 0--1000Hz

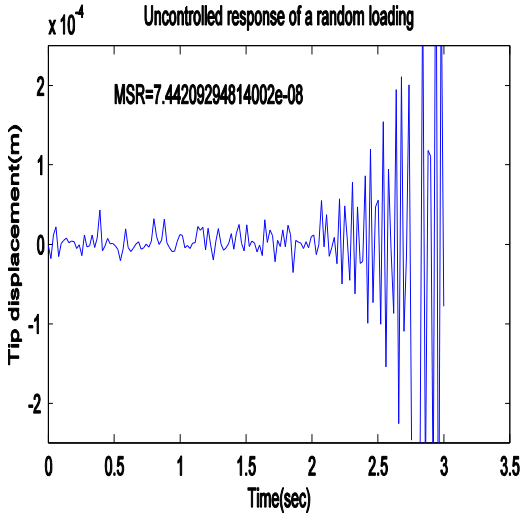

Figure 9: Uncontrolled response of random loading

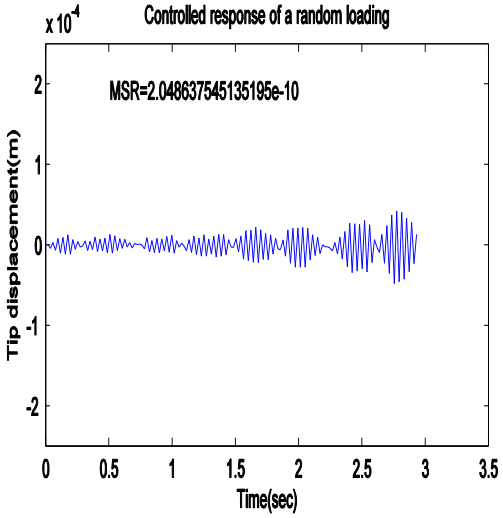

Figure 10: Controlled response of random loading

3.2 Active Buckling Control

The active buckling control of the same smart composite plate with uni-axial compressive load per unit length N_x applied in the x-direction is studied in this case. Table 3 shows the first six buckling loads P_{cr} and Figure 11 shows the first four buckling mode shapes. The controlled results show that the critical buckling load can be increased to the second buckling load (i.e. 210840.66N/m) theoretically which is about 9 times of the first buckling load (i.e. 23483.67N/m). The controlled plate obtains thus enhanced strength compared with the uncontrolled one.

Table 3: First six buckling loads (N/m) for a cantilever composite plate

Mode	1	2	3	4	5	6
P_{cr}	23483.67	210840.66	582420.08	1130344.14	1840004.69	2689188.84

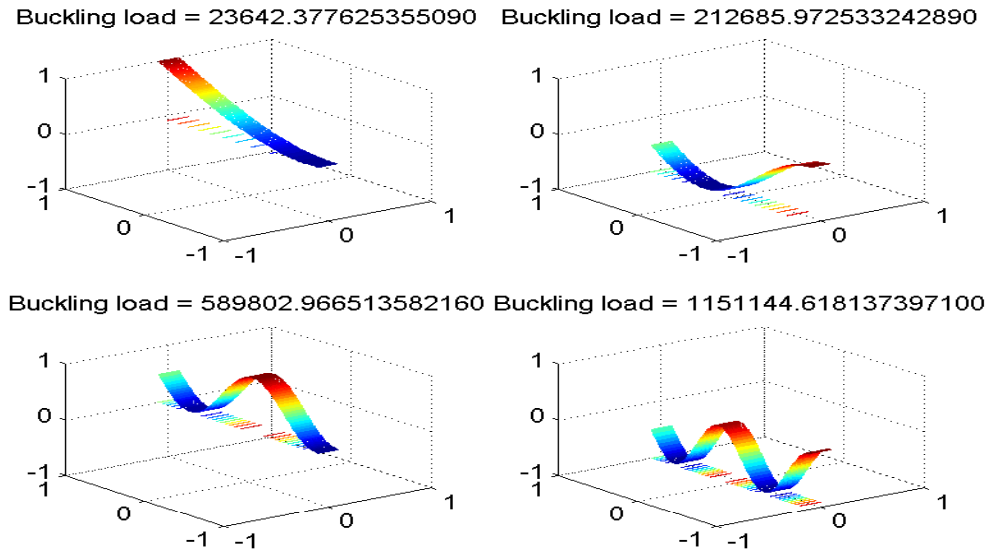

Figure 11: First four buckling modes of a smart composite cantilever plate (N/m)

The weight matrices $Q = C^T C$ and $R = I$, control parameters α and β are kept the same as in the active vibration control design of the last case study. The feedback gain matrix G is computed for an axial load exceeding $P = P_{cr2}$ so that the plate is forced to buckle in the second mode.

Both the one mode minimal model and the first six modes reduced model of the system are studied. Figure 12 shows all the singular values sorted in increasing or decreasing order.

Again the approximate LQG singular values of the six-mode reduced model are the same as the LQG singular values of the structure system so that the six-mode reduced model can accurately represent the full state finite element model. From the sorted LQG compensator singular values, three modes have large contributions to the impulse response of the tip displacement. The minimal realization of the system should include at least these three modes. Two more sensors/actuators segmented pairs are needed to design a full state feedback controller based on this approximate minimal reduced three-mode model.

But from the approximate LQG compensator singular values, only the first mode has a large contribution (about 8 times of the second one) to the impulse response of the tip displacement, thus the other modes can be reduced. Next both the six-mode model and one-mode model are applied for the first buckling mode control design.

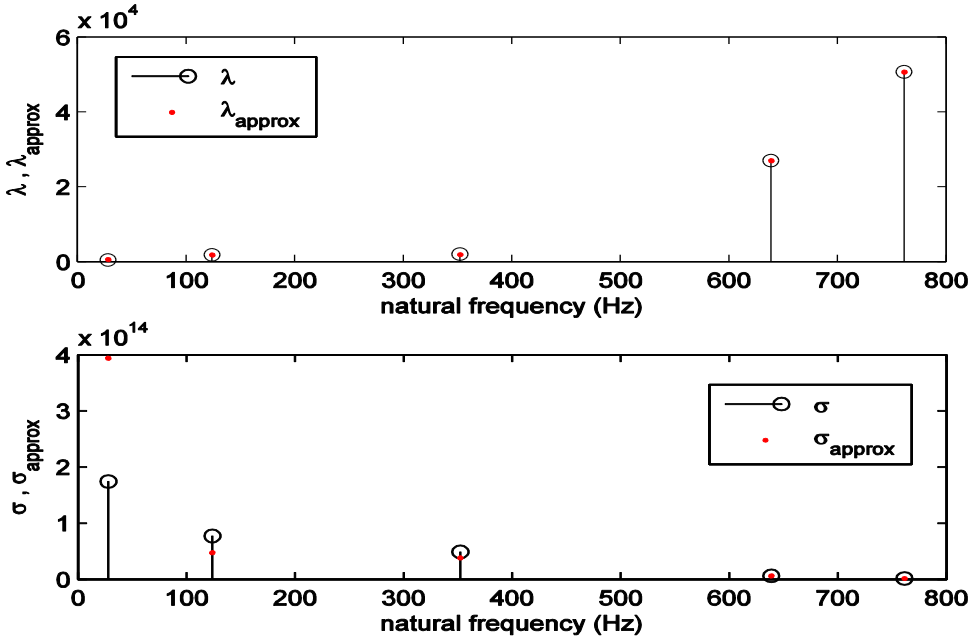

Figure 12: LQG/approximate LQG singular values of system and LQG compensator

The resulting sensor output voltage to a 0.1N impulse load applied on the tip of the plate and the control input voltage of the actuator for the axial compressive load $P = 0.9P_{cr2}$ are shown in figures 13 and 14. The sensor output shows the corresponding voltage outputs in both uncontrolled and controlled cases It is seen that the actuator control voltage in Figure 14 has an absolute value less than the breakdown voltage ($V_{max} = h_a \times 1.0v/\mu m = 100v$) of the piezoelectric PZT-actuator.

The time and frequency responses of the impulse load for the axial compressive load $P = P_{cr2}$ are shown in figures 15 and 16. The time response shows the uncontrolled buckling displacement and controlled stabilizing displacement. It shows that the designed LQR/LQG controller has stabilized the first buckling mode to the second buckling load $P = P_{cr2}$. For comparison, both controlled frequency responses of the two models are shown in Figure 16. Obviously it shows that the only one-mode model cannot control the higher modes.

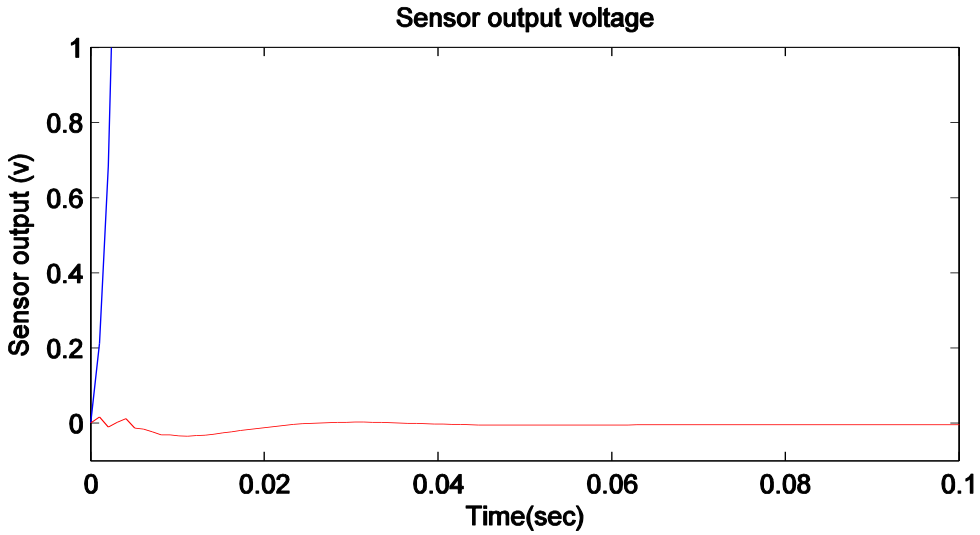

Figure 13: Sensor output voltage of the buckling smart plate

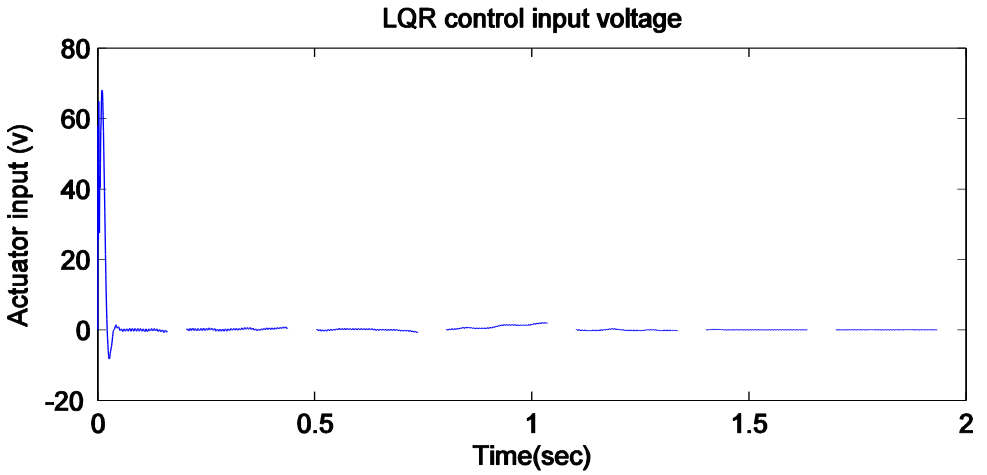

Figure 14: Actuator control input of the buckling smart plate

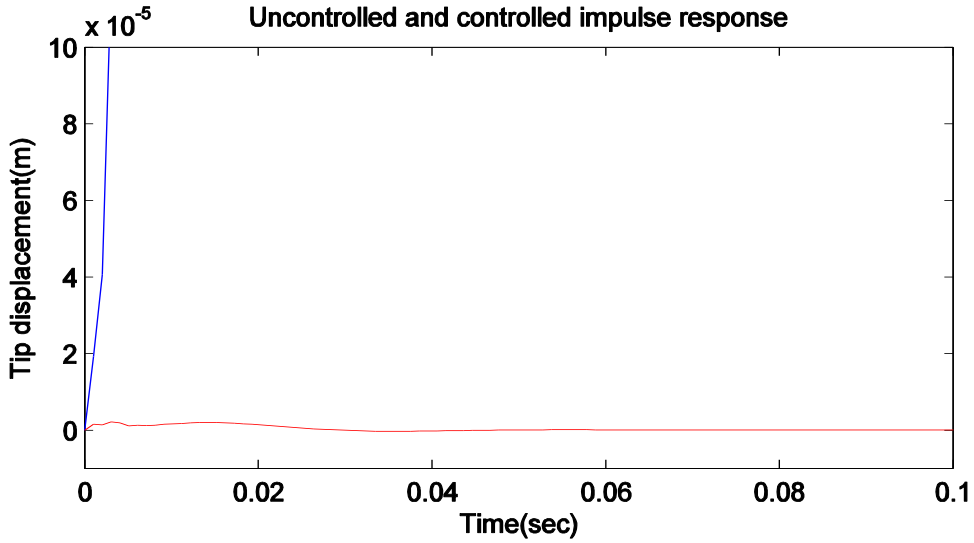

Figure 15: Tip displacement of the buckling smart plate

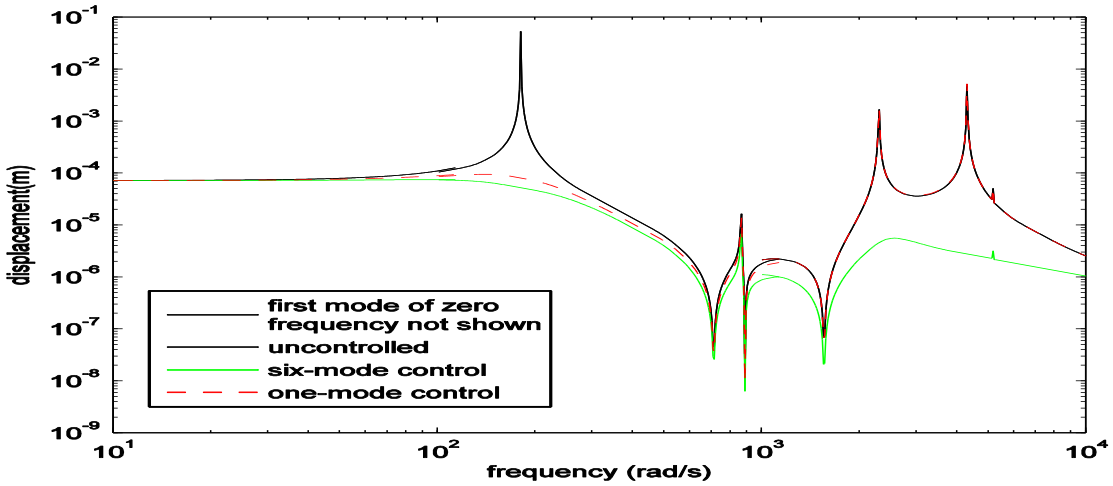

Figure 16: Frequency responses of the buckling smart plate

4 Conclusions

1. Modal model approach with an LQR/LQG control technique gives much more efficient control results to both the vibration suppression and buckling control with the required control voltage in the acceptable range. LQG compensator is also effective in controlling the random vibrations.
2. Model size reduction technique is necessary in the complex structures design to determine the smallest states model while keeping accurate representation of frequency response characteristics. By singular values analysis, the least modes which have the most contributions to the structure system response can be selected to build an approximate reduced modal model.
3. First buckling mode of a cantilever plate has been stabilized by feedback control. Therefore the controlled plate can support a load up to the second buckling load theoretically.

References

Balamurugan, V. and Narayanan, S. 2001, Shell finite element for smart piezoelectric composite plate/shell structures and its application to the study of active vibration control, Finite Elements in Analysis and Design, v37, pp 713-738.
Chandrashekhara, K. and Bhatia, K 1993, Active buckling control of smart composite plates---finite-element analysis, Smart Mater. Structure, 2, 31-39.
Chopra, I. 2002 Review of state of art of smart structures and integrated systems, J.AIAA, V40, No11.
Gawronski, W. 1994, Balanced LQG Compensator for Flexible Structures, Automatica, vol30, 1555–1564.
Kusculuoglu, Z.K., Royston, T.J. 2005, Finite element formulation of composite plates with piezoceramic layers for optimal vibration control applications, Smart Materials and Structures, v14, pp 1139-1153.
Law W.W., W-H Liao, Huang J., 2003, Vibration control of structures with self-sensing piezoelectric actuators incorporating adaptive mechanisms, Smart Materials and Structures, v 12, pp 720-730.
Lewis, F., Syrmos, V.L. 1995, Optimal Control, Wiley, New York.
Meressi, T. and Paden, B. 1993, Buckling control of a flexible beam using piezoelectric actuators. Journal of Guidance, Control, and Dynamics, V.16, No.5, pp977-980.
Narayan, S., Balamurugan, V. 2003, Finite element modeling of piezo-laminated smart structures for active vibration control with distributed sensors and actuators, J. of Sound and Vibration, v 262, 529-562.
Polit, O., Bruant, I. 2006, Electric potential approximations for an eight node plate finite element, Computers and Structures 84, 1480-1493.
Varelis D, Saravanos D.A. 2004, Coupled buckling and post-buckling analysis of active laminated piezoelectric composite plates, Int. J. Solids and Structures, 41, 1519-38.
Wang, Qishan 2012, Active vibration and buckling control of Piezo-electric smart structures, PhD Thesis, McGill University